RESEARCH ARTICLE

The function of CD146 in human annulus fibrosus cells and mechanism of the regulation by TGF-β

Jie Du[1,2] | Wei Guo[1,3] | Sonja Häckel[4] | Sven Hoppe[4] | João P. Garcia[2] | Mauro Alini[1] | Marianna A. Tryfonidou[5] | Laura B. Creemers[2] | Sibylle Grad[1] | Zhen Li[1]

[1]AO Research Institute Davos, Davos, Switzerland

[2]Department of Orthopedics, University Medical Center Utrecht, Utrecht, the Netherlands

[3]Department of Spine Surgery, The First Affiliated Hospital of Sun Yat-sen University, Guangzhou, P. R. China

[4]Department of Orthopaedic Surgery and Traumatology, Inselspital, Bern University Hospital, University of Bern, Bern, Switzerland

[5]Faculty of Veterinary Medicine, Utrecht University, Utrecht, the Netherlands

Correspondence
Laura B. Creemers, Department of Orthopedics, University Medical Center Utrecht, Utrecht, the Netherlands.
Email: l.b.creemers@umcutrecht.nl

Sibylle Grad and Zhen Li, AO Research Institute Davos, 7270 Davos, Switzerland.
Email: sibylle.grad@aofoundation.org (S. G.) and zhen.li@aofoundation.org (Z. L.)

Abstract

The mouse outer annulus fibrosus (AF) was previously shown to contain CD146+ AF cells, while in vitro culture and exposure to transforming growth factor-beta (TGF-β) further increased the expression of CD146. However, neither the specific function of CD146 nor the underlying mechanism of TGF-β upregulation of CD146+AF cells have been elucidated yet. In the current study, CD146 expression and its role in cultured human AF cells was investigated studying the cells' capacity for matrix contraction and gene expression of functional AF markers. In addition, TGF-β pathways were blocked by several pathway inhibitors and short hairpin RNAs (shRNAs) targeting SMAD and non-SMAD pathways to investigate their involvement in TGF-β-induced CD146 upregulation. Results showed that knockdown of CD146 led to reduction in AF cell-mediated collagen gel contraction, downregulation of versican and smooth muscle protein 22α (SM22α), and upregulation of scleraxis. TGF-β-induced CD146 upregulation was significantly blocked by inhibition of TGF-β receptor ALK5, and partially inhibited by shRNA against SMAD2 and SMAD4 and by an Protein Kinase B (AKT) inhibitor. Interestingly, the inhibition of extracellular signal-regulated kinases (ERK) pathway induced CD146 upregulation. In conclusion, CD146 was shown to be crucial to maintain the cell contractility of human AF cells in vitro. Furthermore, TGF-β upregulated CD146 via ALK5 signaling cascade, partially through SMAD2, SMAD4, and AKT pathway, whereas, ERK was shown to be a potential negative modulator. Our findings suggest that CD146 can potentially be used as a functional marker in AF repair strategies.

KEYWORDS
AKT, ALK5, annulus fibrosus, CD146 regulation, cell contractility, SMADs, TGF-β

1 | INTRODUCTION

The intervertebral disc (IVD) consists of a gel-like central structure, the nucleus pulposus (NP), a connective tissue-like outer layer, the annulus fibrosus (AF), and the cartilaginous endplates. Pathologies of the IVD, including herniation and degeneration, are known triggers of chronic low back pain, one of the world leading causes of disability.[1] The AF plays important roles in linking adjacent vertebrae and withstanding mechanical forces, allowing bending, flexion, and torsion of the spine. Acute and chronic injuries of the AF can lead to

IVD degeneration and herniation.[2,3] While discectomy is a common surgical treatment method, unrepaired AF defects after discectomy can lead to reherniation in 10%–30% of cases, which results in recurrent pain and progressive disc degeneration.[4–6] AF repair is a challenge due to its complex structure, high mechanical loading environment, and poor self-healing capability as a virtually avascular tissue.[7] AF cell-based tissue engineering appears to be a promising strategy. Different approaches were taken to repair the AF by using cells alone or in combination with drugs and biomaterials, showing AF cells can orient themselves on biomaterials, proliferate and deposit matrix.[8,9] However, there is a fundamental barrier for clinical translation, which is the limited knowledge about AF cell biology. A better understanding of the populations and phenotypes of AF cells will facilitate the establishment of reparative regeneration strategies to improve AF rupture healing.

Recently, AF cells at the outermost annulus layer of the mouse IVD were found to be cluster of differentiation 146 (CD146) positive, and in vitro positive subpopulations were identified in both human and mouse AF cells.[10] Furthermore, studies confirmed that CD146 has higher expression levels in AF than NP in the human IVD.[11,12] CD146 was identified as a cell adhesion molecule (CAM) in the plasma membrane of human melanoma cells and was thus also named as melanoma cell adhesion molecule (MCAM).[13] CAMs are proteins located on the cell surface that are involved in the process of cell adhesion by binding with other cells or extracellular matrix (ECM).[14] They are highly associated with cell behavior such as cell growth, survival, migration, and differentiation, which are essential for embryonic development and maintaining the integrity of tissue architecture in adults.[15,16] In healthy cells, CD146 is strongly expressed on blood endothelium, smooth muscle, and active T cells, and is defined as a marker of mesenchymal stromal cells (MSCs).[17–21] In the vasculature, CD146 plays crucial roles in vessel structure, angiogenesis, and inflammation.[22] In a variety of carcinomas, accumulating evidence demonstrated that CD146 overexpression may be linked to either the initial development of the primary lesion or progression to metastases.[13,23–25] A high expression of CD146 molecule in bone marrow-derived MSCs is associated with a commitment to a vascular smooth muscle cell lineage characterized by a strong upregulation of muscle protein 22 alpha (SM22α) and an ability to contract collagen matrix.[20] In line with this, also CD146+ AF cells expressed SM22α and demonstrated significantly enhanced contractile properties, although the exact role of CD146 in this enhanced contractility was not investigated.[10]

Expression of CD146 by AF cells was promoted by transforming growth factor-beta (TGF-β), in addition to enhancing ECM synthesis by TGF-β-pretreated AF cells in a bovine whole IVD organ culture model.[26] In fact, induction of CD146 expression by TGF-β has been widely reported in different cell types.[10,26–28] TGF-β increases CD146 expression in progenitor cells originated from human umbilical cord blood and induces their differentiation into vascular smooth muscle cells.[27] In mouse embryonic fibroblasts, TGF-β upregulated CD146 during epithelial mesenchymal transition and activated the extracellular signal-regulated kinases (ERK) pathway and silencing CD146 blocked TGF-β-induced ERK activation.[28] These results indicate that TGF-β-induced activation of ERK is CD146-dependent, although

inhibition of ERK increased CD146 expression, suggesting a feedback mechanism. Upregulation of CD146 by endothelin-3 is Protein Kinase B (AKT) and PI3K-dependent in human melanocytes.[29] CD166 has also been shown to positively regulate CD146 via inhibition of ubiquitin E3 ligases Smurf1 and βTrCP through PI3K/AKT and c-Raf/MEK/ERK signaling in Bel-7402 hepatocellular carcinoma cells.[30] However, which pathway plays the most important role in TGF-β-induced CD146 upregulation in AF cells is still unknown.

The current study aims to investigate the function of CD146 and the TGF-β signaling pathway underlying the upregulation of CD146 in human AF cells. The multiple functions of CD146 were investigated by short hairpin RNA (shRNA) knockdown of *CD146* in human AF cells. Cell contractility and gene expression of various functional phenotype markers of AF cells were evaluated. Furthermore, we interfered with the SMAD and non-SMAD TGF-β signaling pathways to elucidate the mechanism behind TGF-β-induced CD146 expression.

2 | MATERIALS AND METHODS

2.1 | Human AF cells isolation and expansion

Human AF tissue was obtained with written consent from waste tissue of traumatic IVDs (six donors, Inselspital Bern). The Swiss Human Research Act does not apply to research which involves anonymized biological material and/or anonymously collected or anonymized health-related data. Therefore, this project does not need to be approved by the ethics committee. General Consent which also covers anonymization of health-related data and biological material was obtained. Intact IVDs (two donors, University Medical Center Utrecht) were obtained as part of the standard postmortem procedure as approved by the medical ethics committee of the University Medical Center Utrecht (METC No. 12-364). Donors age was from 19 to 61, mean age 35, and disc degeneration level was classified on magnetic resonance imaging (MRI) or naked eyes (Pfirrmann grade II [four donors], I [two donors], no information [two donors]) (Table S1). The isolation and expansion methods of human AF cells have been described previously.[26] Briefly, after removing adjacent NP and cartilaginous endplate, the purified AF tissue was incubated with 20 ml red blood cell lysis buffer (155 mM NH$_4$Cl, 10 M KHCO$_3$, and 0.1 mM EDTA in ultrapure water) for 5 min at room temperature. Then, minced tissue was first digested for 1 h with 0.2% w/v Pronase (Roche) in αMEM (Gibco), followed by 12–14 h at 37°C in 130 U/ml collagenase type II (Worthington) in αMEM with 10% fetal bovine serum (FBS, PAN Biotech). Single cells were washed once with expansion culture medium (αMEM supplemented with 10% FBS, 100 U/ml penicillin and 100 mg/ml streptomycin [1% P/S, Gibco]), then seeded at a concentration of 10,000 cells/cm^2 and expanded. AF cells were cultured at a hypoxic condition at 2% O$_2$, 5% CO$_2$, at 37°C. Culture medium was changed twice a week. Cells were passaged at a ~ 80% confluency, detached by 0.05% trypsin/EDTA (Gibco) with 0.01% collagenase P (Roche) for 5 min at 37°C. Cells were frozen at Passage 1 for further use.

2.2 | AF cells treatment with TGF-β1 and pathway inhibitors

AF cells at Passage 1 were thawed, seeded in T150 flasks at 0.5×10^6 cells per flask and expanded in expansion culture medium until passage 2. At ~80% confluence, cells were subcultured to Passage 3 at a ratio of 1:4 to T75 flasks. When cells were ~60% confluent, they were treated with or without inhibitors in either basal medium (αMEM supplemented with 5% FBS, 1% P/S, 1% ITS + [BD Biosciences]) or TGF-β medium (basal medium supplemented with 5 ng/ml of TGF-β1 [Fitzgerald]) for 2 days. After treatment, cells were detached. Half of the cells were used for flow cytometry analysis, and the remaining cells were used for RNA isolation and gene expression analysis. The inhibitors used in current study are listed in Table 1.

2.3 | Cell treatment with shRNA-lentivirus

AF cells were transfected with shRNA-lentivirus at Passage 3. Briefly, single cell and virus suspensions were prepared at a concentration of 0.5×10^5 cells/ml and 2×10^6 TU/ml, respectively within transfection medium (αMEM supplemented with 10% FBS, 1% P/S, 5 µg/ml polybrene [VectorBuilder]). Transfection was performed by mixing single cell and virus suspension at a ratio v- v = 1:2. Cells and virus mixture were then seeded and incubated for 24 h at hypoxic condition. All the shRNA-lentiviruses were bought from VectorBuilder, US. ShCD146 was labeled with Enhanced Green Fluorescent Protein (EGFP), sequence 5′-TTCCTGGAGCTGGTCAATTTA-3′; ShSMAD4 was labeled with EGFP, sequence 5′-GCCAGCTACTTACCATCATAA–3′; ShSMAD2 was labeled with mCherry, sequence 5′-CAAGTACTCCTTG CTGGATTG-3′; ShScrambled was labeled with EGFP. For flow cytometry and gene expression analysis, cells and virus mixture were seeded in six-well plate at 1.5 ml per well. After a 24 h transfection, cells were treated with basal medium or TGF-β medium for another 2 days. For the cell contractility assay, transfection was performed in 100 mm culture dish with 9 ml mixture. After 24 h incubation, transfection medium was refreshed with culture medium for another 24 h, where after cells were detached and seeded into Collagen I gel (from rat tail, Corning). Transfection efficiency was estimated under fluorescence microscope (Supporting Information Data 1).

2.4 | Flow cytometry analysis

Treated cells were detached and suspended in 100 µl staining buffer: phosphase buffered saline (PBS) with 0.2% bovine serum albumin (BSA) and 1 mM EDTA. Cell suspensions were incubated with 5 µl fluorescence-conjugated mouse monoclonal anti-human CD146 antibody (CD146-APC, Miltenyi Biotec) at final concentration 5 µg/ml or the same amount of IgG1-APC (isotype control, Miltenyi Biotech) in the dark for 30 min at 4°C. After incubation and washing, 4′,6-diamidino-2-phenylindole (DAPI) or Propidium Iodide was used for dead cell staining at a final concentration of 0.1 µg/ml (AKT inhibitor,

TABLE 1 List of TGF-β pathway inhibitors

Inhibitor	Source	Target	Solvent	Used concentration
MK-2206 2HCl	Selleckchem	AKT	DMSO	1 µM[31]
SB525334	Selleckchem	ALK5	DMSO	1 µM[32]
BIRB 796	Selleckchem	P38	DMSO	1 µM[33]
SCH 772984	Selleckchem	ERK1/2	DMSO	1 µM[34]
SP 600125	Selleckchem	JNK	DMSO	10 µM[35]
SIS3 HCl	Selleckchem	SMAD3	DMSO	3 µM[36]
Y-27632	Sigma	ROCK	DMSO	1 µM[37]

Abbreviation: AKT, Protein Kinase B; DMSO, dimethyl dulfoxide; ERK, extracellular signal-regulated kinases; TGF-β, transforming growth factor-beta.

MK-2206 2HCl, has autofluorescence and interferes with DAPI channel; thus Propidium Iodide was used to label dead cells for cells treated with AKT inhibitor). Flow cytometric analysis was performed on a FACS AriaIII (BD Biosciences) and at least 30,000 events per sample were recorded. Data analysis was performed using BD FACSDiva software. A gating strategy was used to exclude dead cells and cell doublets. In lentivirus-transfected cells, the percentage of CD146$^+$ cells was calculated in the transfection positive cell fraction, identified by labeling of fluorescent protein EGFP and mCherry.

2.5 | Cell contractility assay

The cell contractility assay was performed with shCD146 and scramble transfected AF cells from three donors. Cells were encapsulated in 1.81 mg/ml Type I collagen at a seeding density of 1×10^5 cells/ml. The collagen gel was seeded in 24-well precoated 1% BSA plates at 0.5 ml per well with four technical replicates and incubated at 37°C for at least 1 h. After gelling, gels were cultured expansion culture medium with or without TGF-β1 5 ng/ml at hypoxia condition. Gels were photographed on Day 1, 4, 7 after seeding. The diameter of the gels was measured by ImageJ 1.53c. Gel diameters were averaged to calculate diameter change with the formula $D_{well} - D_{gel}/D_{well}$ (D_{well}: diameter of well, D_{gel}: diameter of gel), and the diameter change was normalized to Day 1 scramble by donor, whereby greater change equaled with higher contractility. This method was modified from a previous study.[10]

2.6 | RNA isolation and quantitative real-time PCR

RNA isolation was performed using TRI reagent (Molecular Research Center Inc.) with polyacryl carrier (Molecular Research Center Inc.) at a ratio v: v = 200: 1 according to the manufacturer's protocol. Phase separation was performed by adding 100 µl bromo-chloropropane per 1 ml of TRI reagent. The aqueous phase after centrifugation was transferred to a fresh tube and mixed with 250 µl of isopropanol

followed by 250 μl of high salt precipitation solution (MRC) per 1 ml of TRI reagent. After precipitation and washing, RNA was dissolved in diethylpyrocarbonate-treated water and quantified by NanoDrop 1000 (Thermo Scientific). Reverse transcription was performed using SuperScript® VILO™ cDNA Synthesis Kit (Invitrogen) with 500 ng total RNA. Quantitative real-time PCR was conducted on Quant-Studio6 System (Applied Biosystems). Sequences of the primers and probes used in qRT-PCR are listed in Table 2. RPLP0 ribosomal RNA was used as endogenous control. Data were analyzed using the $2^{-\Delta\Delta C_t}$ method.

2.7 | Western blot

Cells transfected with shSMAD2, shSMAD4, or both were cultured in 100 mm dish and scramble was transfected as control. At 80% confluency, cells were treated with basal medium or TGF-β medium for 1 h. Cell lysis was carried out by radioimmunoprecipitation assay buffer (Sigma-Aldrich, R0278) with protease inhibitor cocktail (Sigma, P8340) and phosphatase inhibitors, PhosSTOP™ (Sigma-Aldrich). Protein concentration was determined using the Bicinchoninic Acid (BCA) protein assay method, with BCA Solution (Sigma), Copper (II) Sulfate Solution (Sigma-Aldrich), Serum Albumin Standard (Bio-Rad), then mixed with a 5× sample buffer (GeneScript). The samples were loaded at 10 μg total protein, separated by electrophoresis in 8% Sodium dodecyl-sulfate polyacrylamide gel electrophoresis (SDS-PAGE), transferred to nitrocellulose membranes (0.45 μm), hybridized with corresponding antibodies, detected using the SuperSignal™ West Dura Extend Duration Substrate (Thermo Scientific, 34075), and photographed by ChemiDoc® Touch Imaging system (BIO-RAD). Primary antibodies included rabbit anti-human SMAD2/3 (Cell Signaling, #8685), rabbit anti-human SMAD2 (Cell Signaling, # 5339) and rabbit anti-human Phospho-SMAD2 (Ser465/467) (Cell Signaling, #3108), were diluted in 5% BSA in PBS (PBS-BSA) at v: v = 1:1000; endogenous control, mouse anti-human GAPDH (Abcam, ab9484) and mouse anti-human γ-tubulin (Sigma, T6557) diluted in PBS-BSA at v: v = 1:3000. Secondary antibodies polyclonal rabbit anti-mouse-HRP (Dako, P0260) and polyclonal swine anti-mouse-HRP (Dako, P0217) were diluted in 5% nonfat milk in PBS at v: v = 1:2000.

2.8 | Statistical analysis

Statistical analyses were performed using the IBM SPSS statistics software, version 20.

One-sample Wilcoxon test versus "1" was used to determine the difference of CD146 expression upon treatment with shSMADs and inhibitors. One-way analysis of variance (ANOVA) was used to determine the differences between two groups with Bonferroni (homogeneity variance) or Dunnett T3 (non-homogeneity variance) post hoc testing. $p < 0.05$ was considered statistically significant.

TABLE 2 List of oligonucleotide primers and probes used for quantitative real-time PCR

Gene	Primer/ probe type	Sequence
COL1A1	Primer fw (5′–3′)	CCC TGG AAA GAA TGG AGA TGA T
	Primer rev (5′–3′)	ACT GAA ACC TCT GTG TCC CTT CA
	Probe (5′FAM/3′ TAMRA)	CGG GCA ATC CTC GAG CAC CCT
COL2A1	Primer fw (5′–3′)	GGC AAT AGC AGG TTC ACG TAC A
	Primer rev (5′–3′)	GAT AAC AGT CTT GCC CCA CTT ACC
	Probe (5′FAM/3′ TAMRA)	CCT GAA GGA TGG CTG CAC GAA ACA TAC
ACAN	Primer fw (5′–3′)	AGT CCT CAA GCC TCC TGT ACT CA
	Primer rev (5′–3′)	CGG GAA GTG GCG GTA ACA
	Probe (5′FAM/3′ TAMRA)	CCG GAA TGG AAA CGT GAA TCA GAA TCA ACT
MMP3		Hs00968305_m1
ADAMTS5		Hs01095518_m1
CD146		Hs00174838_m1
SM22α		Hs00162558_m1
SCX		Hs03054634_g1
MKX		Hs00543190_m1
ELN		Hs00355783_m1
VCAN		Hs00171642_m1
RPLP0	Primer fw (5′–3′)	TGG GCA AGA ACA CCA TGA TG
	Primer rev (5′–3′)	CGG ATA TGA GGC AGC AGT TTC
	Probe (5′FAM/3′ TAMRA)	AGG GCA CCT GGA AAA CAA CCC AGC

Note: Primers and probes with the sequence shown were custom-designed; primers and probes with the catalog number were from Applied Biosystems.

Abbreviations: ACAN, Aggrecan; ADAMTS5, A Disintegrin and Metalloproteinase with Thrombospondin Motifs 5; CD146, Cluster of Differentiation 146; COL2A1, Type II Collagen; COL1A1, Type I Collagen; ELN, Elastin; fw, Forward; FAM, Carboxyfluorescein; MMP3, Matrix Metalloproteinase-3; MKX, Mohawk Homeobox; rev, Reverse; RPLP0, Ribosomal Protein Lateral Stalk Subunit P0; SM22α, Smooth Muscle Protein 22-alpha; SCX, Scleraxis; TAMRA, Tetramethylrhodamine; VCAN, Versican.

3 | RESULTS

3.1 | CD146 knockdown impairs the contractility of human AF cells

To evaluate the role of CD146 in cell contractility, shCD146 lenti-virus was used to silence *CD146* in human AF cells cultured with

basal and TGF-β media. Transfection efficiency was estimated to be more than 50% using fluorescence microscope (Supporting Information Data 1). Cell viability, evaluated by Alamar Blue Assay, was decreased after transfection with lentivirus, but no differences were observed between scramble and shCD146 (Supporting Information Data 2).

As shown in Figure 1A, the percentage of CD146$^+$ cells was upregulated by TGF-β ($p < 0.001$), and it was significantly decreased by shCD146 when cultured with ($p < 0.001$) and without TGF-β ($p < 0.01$) compared with scramble. Likewise, the relative $CD146$ mRNA expression levels in shCD146-treated cells was significantly downregulated when compared with scramble in basal ($p < 0.01$) and TGF-β ($p < 0.05$) media (Figure 1B). Altogether, these results confirm shCD146-mediated knockdown of CD146 at the gene and protein level in both baseline expression and TGF-β-induced upregulation.

Cell contractility assay was performed in three donors and measured at different timepoints. As shown in Figure 1C,D, the gels contracted with time, and this contraction was enhanced by TGF-β (Day 1 $p < 0.05$, Day 4 $p < 0.01$, Day 7 $p = 0.055$). Interestingly, this contraction was inhibited by shCD146 independently of time. The diameter change was significantly smaller in shCD146 compared with scrambled shRNA with (Day 1 $p < 0.001$, Day

4 $p < 0.001$, Day 7 $p < 0.01$) or without (Day 1, Day 4, and Day 7, $p < 0.001$) TGF-β at each time point.

3.2 | CD146 is associated with the expression of AF marker genes

Several genes that are associated with AF function and phenotype were evaluated after $CD146$ silencing, including ECM genes ($ACAN$, $COL1A1$, $COL2A1$, $VCAN$, ELN), catabolic genes of ECM ($MMP3$, $ADAMTS5$), and tendon/ligaments-related genes ($SM22\alpha$, SCX and MKX) (Figure 2). In AF cells treated with TGF-β and scramble shRNA, $SM22\alpha$ ($p < 0.01$) and SCX ($p < 0.01$) were significantly upregulated, and $ACAN$ ($p < 0.01$), MKX ($p < 0.05$), $MMP3$ ($p < 0.05$), and $ADAMTS5$ ($p < 0.001$) were significantly downregulated compared with nontreated controls. The expression level of $VCAN$ was significantly decreased by shCD146 in absence ($p < 0.001$) and presence ($p < 0.001$) of TGF-β compared with scramble. $SM22\alpha$ was downregulated by shCD146 in absence ($p < 0.001$), but not in the presence of TGF-β. However, the expression of SCX was significantly upregulated by shCD146 in absence ($p < 0.001$) of TGF-β, but not significant in the presence ($p = 0.066$) of TGF-β. $ADAMTS5$ was upregulated by shCD146 compared with scramble in the presence of TGF-β ($p < 0.05$).
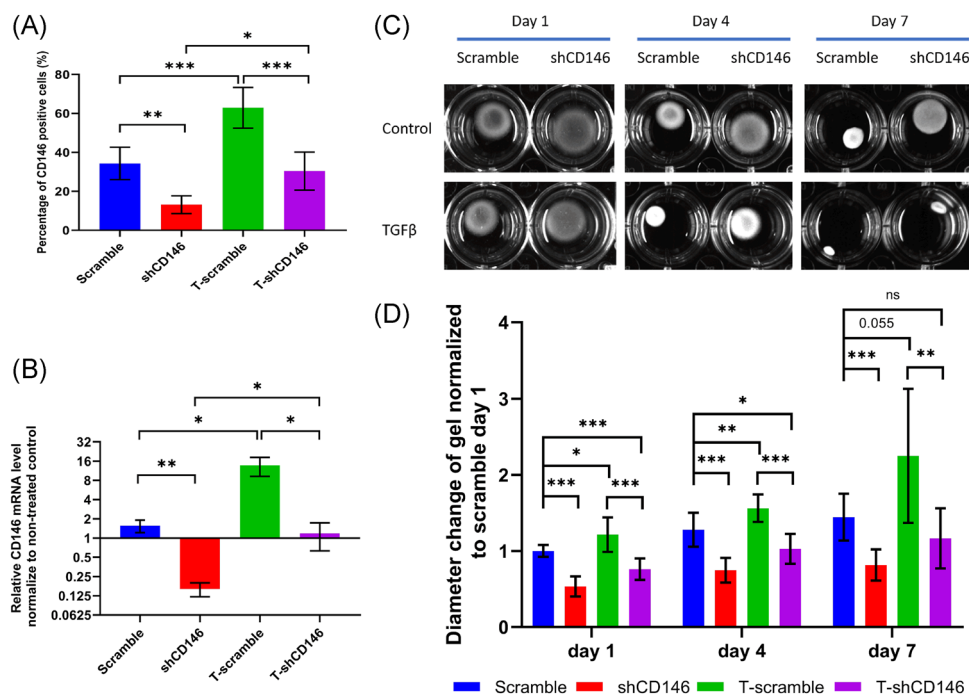

FIGURE 1 Cell contractility assay performed in $CD146$ knockdown AF cells. $CD146$ was knocked down by shCD146 transfection, scramble served as control, and cultured with basal medium (Scramble, shCD146) or TGF-β medium (T-scramble, T-shCD146). (A) Percentage of CD146$^+$ cells and (B) mRNA expression level normalized to cells which were nontransfected and cultured with basal medium (Scramble, shCD146) or TGF-β medium (T-scramble, T-shCD146). Mean ± SD, $n = 5$. (C,D) Cell contractility assay performed in collagen Type I gels in three donors with four replicates after $CD146$ knockdown. (C) Macroscopic images of gels, (D) quantified diameter change of gels normalized to Day 1 Scramble (Mean ± SD, $n = 12$). Statistical analysis performed using one-way ANOVA with Bonferroni (homogeneity variance) or Dunnett T3 (non-homogeneity variance) post-hoc testing. AF, annulus fibrosus; ANOVA, analysis of variance; TGF-β, transforming growth factor-beta. *$p < 0.05$, **$p < 0.01$, ***$p < 0.001$

3.3 | Investigation on signaling pathways of TGF-β-induced CD146 upregulation

The above-mentioned results show that TGF-β treatment induced CD146 upregulation in human AF cells. However, the underlying mechanism is not known yet. TGF-β signaling pathways generally include SMAD pathways and non-SMAD pathways, also known as canonical and noncanonical pathways. In this study, we studied the TGF-β-induced signaling cascade employing the inhibitor targeting TGF-β receptor type I, activin receptor-like kinases 5 (ALK5). Furthermore, inhibition of SMAD pathways was performed using SMAD3 inhibitor and shRNA targeting SMAD1, SMAD2, and SMAD4. Inhibitors targeting AKT, ERT, P38, JNK, and ROCK were also utilized to block non-SMAD pathways.

3.3.1 | TGF-β upregulates CD146 via TGF-β receptor Type I, ALK5

When treated with iALK5 the percentage of CD146+ AF cells was significantly decreased in basal medium ($p < 0.05$) and TGF-β medium ($p < 0.05$) compared with nontreated control (Figure 3A,B). The mRNA level of CD146 was significantly reduced by iALK5 in TGF-β medium ($p < 0.05$), but not in basal medium ($p = 0.075$) compared with nontreated control (Figure 3B). These results indicate that TGF-β-induced CD146 upregulation is ALK5 dependent.

3.3.2 | TGF-β upregulates CD146 partially via SMAD4–SMAD2 pathways

AF cells were transfected with shSMAD2 and shSMAD4, whereby the transfection efficiency was more than 50% (Supporting Information

Data 1). Cell viability was decreased by transfection, but less affected by shSMAD4 compared with scramble (Supporting Information Data 2). SMAD2 and SMAD4 were significantly downregulated by shSMAD2 and shSMAD4, respectively, at both the protein (Figure 4A) and mRNA level ($p < 0.001$) (Figure 4B). The phosphorylation of SMAD2 was also downregulated by shSMAD2 in medium with or without TGF-β (Figure 4A). Knockdown of SMAD2 reduced CD146 expression, as indicated by lower percentage of CD146+ cells and CD146 mRNA level in basal and TGF-β media compared with scramble ($p < 0.05$) (Figure 4C,D). Knockdown of SMAD4 led to lower percentage of CD146 + cells, decreased CD146 expression in basal condition compared with scramble ($p < 0.05$), lower percentage of CD146+ cells ($p < 0.05$), but not change of mRNA level in TGF-β condition compared with scramble. Simultaneous knockdown of SMAD2 and SMAD4 was performed in two independent donors. However, there was no further reduction in expression of CD146 compared with individual knockdown (Supporting Information Data 3). Cells were also treated with SMAD3 inhibitor or transfected with shSMAD1, which did not show any inhibition of TGF-β-induced CD146 upregulation (Supporting Information Data 4). Taken together, TGF-β highly upregulated CD146, as indicated by increased percentage of CD146+ cells and CD146 gene expression in human AF cells. This upregulation was partly neutralized by blocking SMAD4-SMAD2 pathways. However, there was no effect when blocking SMAD3 or SMAD1. These results indicate that TGF-β, if at all, only partially upregulates CD146 via SMAD4-SMAD2 pathways.

3.3.3 | The AKT and ERK pathways play roles in regulation of CD146 expression

AF cells were treated with non-SMAD signaling pathway inhibitors in media supplemented with or without TGF-β. Inhibitors targeting
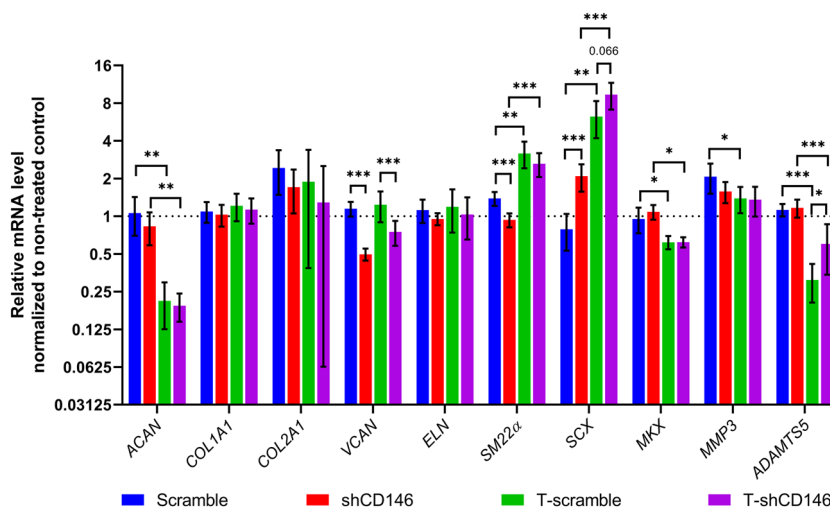

FIGURE 2 Gene expression of AF cells after CD146 silencing. Relative mRNA expression of AF cells transfected with shCD146, scrambled shRNA as control, and cultured with basal medium (Scramble, shCD146) or medium containing TGF-β (T-scramble, T-shCD146) in three donors. Data were normalized to expression level of cells which were nontransfected and cultured with basal medium. Statistical analysis performed using one-way ANOVA with Bonferroni (homogeneity variance) or Dunnett T3 (nonhomogeneity variance) post hoc testing. Mean ± SD, $n = 8$. AF, annulus fibrosus; ANOVA, analysis of variance; TGF-β, transforming growth factor-beta. *$p < 0.05$, **$p < 0.01$, ***$p < 0.001$
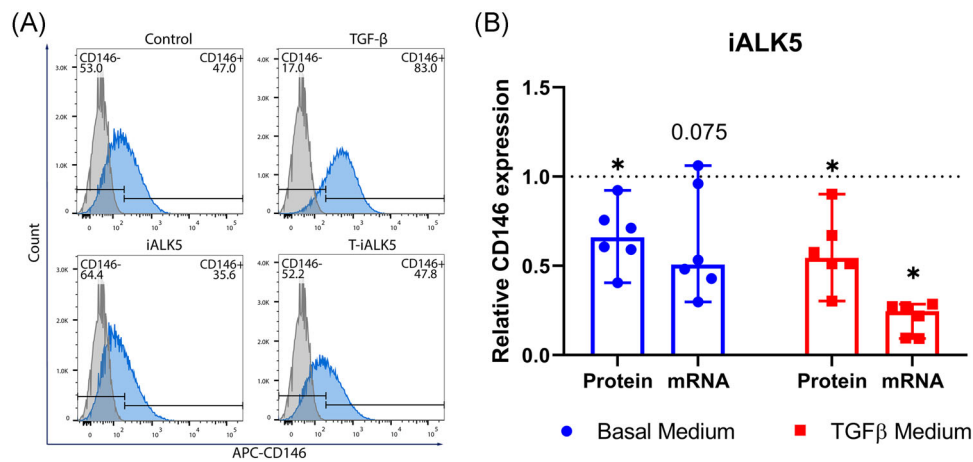
FIGURE 3 Expression of CD146 after treatment with TGF-β receptor type I (ALK5) inhibitor. ALK5 was blocked using a specific inhibitor and cultured with basal medium (Control, iALK5) or TGF-β medium (TGF-β, T-iALK5). (A) The percentage of CD146$^+$ cells (protein) was measured by flow cytometry. (B) CD146 mRNA level was analyzed by qRT-PCR. Results were normalized to nontreated control in basal and TGF-β medium separately. Statistical analysis performed by using one-sample Wilcoxon versus "1". Median with 95% CI, $n = 6$, *$p < 0.05$. qRT-PCR, quantitative real-time polymerase chain reaction; TGF-β, transforming growth factor-beta

ROCK, p38, and JNK did not show any regulatory effect on the TGF-β-induced upregulation of *CD146* (Supporting Information Data 4). When treated with AKT inhibitor, the percentage of CD146$^+$ cells and *CD146* mRNA showed a decrease in basal medium and TGF-β medium compared with nontreated control ($p < 0.05$) (Figure 5A,B). Interestingly, the percentage of CD146$^+$ cells significantly increased when cells were treated with ERK inhibitor in basal medium ($p < 0.05$), and the same trend was observed in TGF-β medium ($p < 0.05$) (Figure 5C,D). The *CD146* mRNA level was comparable between iERK-treated and nontreated groups cultured with both media (Figure 5D). These results indicate that AKT and ERK signaling pathways may play a role in the regulation of *CD146* expression in baseline and TGF-β-induced upregulation, whereby AKT may be a positive modulator, while ERK may be a negative modulator.

4 | DISCUSSION

In the current study, we evaluated the role of CD146 in human AF cells, and partly elucidated the mechanisms underlying TGF-β-mediated upregulation of CD146. Our results showed that CD146 was required for contractility of human AF cells. Knockdown of CD146 impaired cell contractility in collagen I hydrogel, which is the major component of AF ECM. These results indicated that CD146 may be a modulator of cell–matrix interaction in AF and a potential marker for AF tissue engineering; self-assembly of aligned tissue-engineered AF composite via collagen gel contraction could be used to create a mechanically functional tissue-engineered IVD.[38] Also in vascular smooth muscle cells, enhanced contractility and mobility mediated by SM22a, was crucial for maintaining their differentiated phenotype.[39] In a previous study, CD146$^+$ AF cells showed better contractility and higher expression of SM22α and elastin in mouse.[10] In line with these results, we showed that CD146 knockdown caused

downregulation of *SM22α*, albeit not of elastin, in human AF cells. This suggests that CD146 contributes to the development of a contractile phenotype by upregulating *SM22α*, but not elastin in human AF cells.

CD146 can also be implicated in ECM remodeling. VCAN, a large proteoglycan present in ECM and expressed in both NP and AF, has been shown to be elevated at early stages of degeneration and to decrease in severely degenerated tissues.[40] The mRNA expression of *VCAN* was decreased by *CD146* silencing which indicates that *CD146* may be a positive modulator of *VCAN*. Interestingly, when *CD146* was upregulated by TGF-β, *VCAN* was not. These results indicate that the expression of *VCAN* may not be only CD146-dependent. Furthermore, TGF-β led to a reduction of *ADAMTS5* expression, and this effect was partly neutralized by *CD146* knockdown. These findings indicate a potential role of CD146 in ECM turnover and AF contractility, although the contribution of proteoglycans to the ECM in the hydrogel was likely limited.

Blocking *CD146* expression increased the TGF-β-dependent and independent expression of *SCX*, pointing toward an interaction between *CD146* and *SCX*. SCX is a marker of tendon and ligaments cells and deletion of SCX leads to severely hypoplastic long-range tendons, and causes defective maturation of tendons, ligaments, and the outer AF.[41–43] In tendon, SCX plays important roles in progenitor cell proliferation, tenogenic differentiation, and maturation,[44,45] while CD146 is a maker of progenitor cells with powerful capability for tendon regeneration.[44,46] A recent study showed that the loss of regeneration potential of AF cells in adult mice is accompanied with lower SCX expression compared with neonatal mice.[47] CD146$^+$ AF cells showed comparable multiple differentiation potential and weaker cell proliferation capacity than CD146$^-$ AF cells.[10] Altogether, in tendon progenitor cells, the expression of SCX and CD146 indicates a potential for tendon regeneration; while in AF cells, the expression of SCX may suggest a stem cell probability, and the
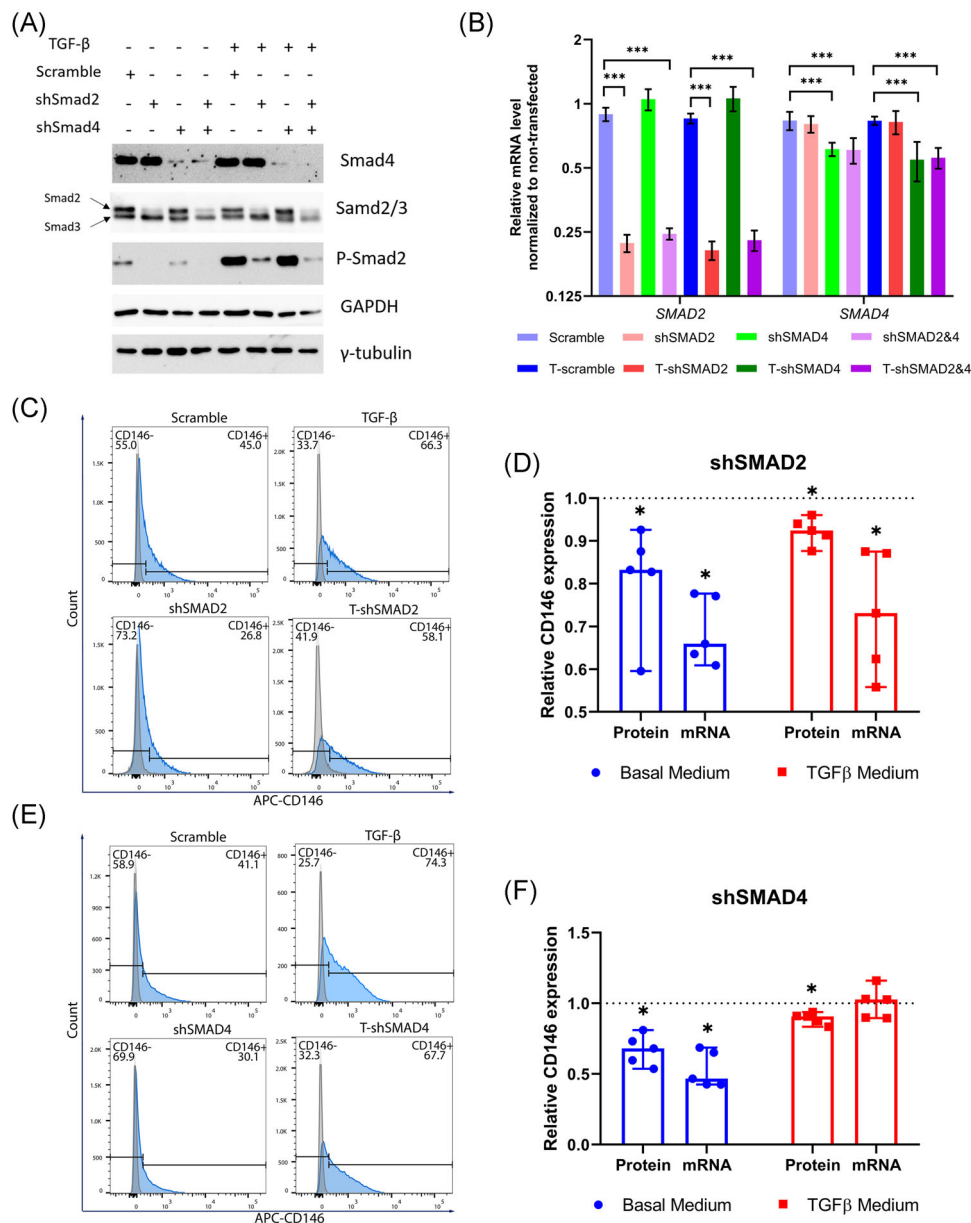
FIGURE 4 Expression of CD146 after blocking SMAD4-SMAD2 pathway. *SMAD2* and *SMAD4* were knocked down by shSMAD2 or/and shSMAD4 transfection, scramble as control, and cultured with basal (Scramble, shSMAD2, shSMAD4, shSMAD2&4) or TGF-β medium (T-Scramble, T-shSMAD2, T-shSMAD4, T-shSMAD2&4). (A) The protein level of SMAD4, SMAD2/3, and P-SMAD2 (phosphorylation of SMAD2) examined by Western Blot. (B) The mRNA expression of *SMAD2* and *SMAD4* measured by qRT-PCR (mRNA was normalized to expression level of cells which were nontransfected control), statistical analysis performed by using one-way ANOVA with Bonferroni (homogeneity variance) or Dunnett T3 (nonhomogeneity variance) post hoc testing. Mean ± SD, $n = 6$, ***$p < 0.001$. (C,E) The percentage of CD146$^+$ cells (protein) measured by flow cytometry after knockdown *SMAD2* and *SMAD4*. (D,F) *CD146* mRNA level analyzed by qRT-PCR after knockdown *SMAD2* and *SMAD4*. Results were normalized to scramble in basal and TGF-β media separately. Statistical analysis performed by using one-sample Wilcoxon test versus "1". Median with 95% CI, $n = 5$, *$p < 0.05$. ANOVA, analysis of variance; qRT-PCR, quantitative real-time polymerase chain reaction; TGF-β, transforming growth factor-beta

expression of CD146 may indicate a mature AF cells phenotype. The phenotype induced by TGF-β with upregulation of *SCX* and *CD146* tend to be a mature differentiated cell type in cultured AF cells, namely, TGF-β maintains differentiation of AF cells during in vitro expansion. Hereby, we report for the first time *SCX* expression is regulated by *CD146*. Whether this regulation is related to

differentiation and regeneration of tendon and AF needs further investigation.

Altogether these findings indicate that CD146 may be involved in AF function. The expression of CD146 is known to be regulated by several factors, including proinflammatory factors and growth factors, such as tumor necrosis factor alpha (TNF-α),[48] interleukin−13
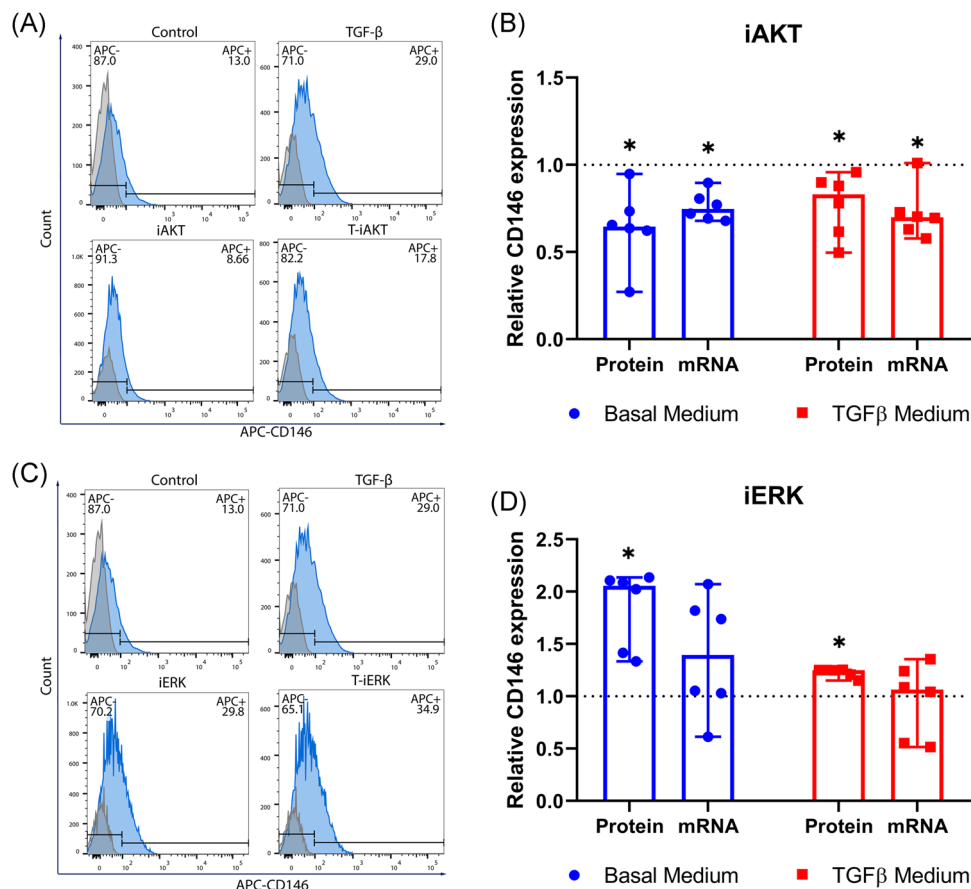
FIGURE 5 Expression of CD146 after blocking AKT and ERK pathways. The percentage of CD146+ cells and the *CD146* mRNA level of AF cells treated with (A,B) AKT and (C,D) ERK inhibitors and cultured with basal medium (Control, iAKT, iERK) or TGF-β medium (TGF-β, T-iAKT, T-iERK). (A,C) The percentage of CD146 + cells (protein) was measured by flow cytometry. (B,D) *CD146* mRNA level was analyzed by qRT-PCR. Results were normalized to nontreated control in basal and TGF-β medium separately. Statistical analysis performed by using one-sample Wilcoxon versus "1". Median with 95% CI, $n = 6$, *$p < 0.05$. TGF-β, transforming growth factor-beta

(IL-13),[49] TGF-β1, or bone morphogenetic protein 4 (BMP4).[28] Our results showed the upregulation of CD146 by TGF-signaling in human AF cells was partially mediated by ALK5. ALK5 is one of the TGF-β type I receptors which propagates the extracellular signals with TGF-β type II receptor via phosphorylation of mediators, and activation of SMAD and non-SMAD signaling pathways.[50,51] ALK5 can mediate TGF-β signaling by activating Smad2/3 in most cell types, while in endothelial cells ALK1 activates Smad1/5/8 for TGF-β signaling.[52,53] In the current study, CD146 expression by AF cells in baseline and TGF-β-induced upregulation was modulated via ALK5-SMAD2/4 cascade, but SMAD3 and SMAD1 seem not to be involved.

Besides the SMAD pathways, non-SMAD pathways play an important role in TGF-β signaling. Here we showed that TGF-β may upregulate CD146 via AKT, rather than the JNK, p38 or ROCK pathways. Previous studies showed endothelin-3 promoted CD146 expression via PI3K/AKT in melanocytes,[29] and PI3K/AKT and c-Raf/MEK/ERK positively regulated CD146 via inhibition of its ubiquitination and degradation in hepatoma cell.[30] Interestingly, in the present study, inhibition of the ERK pathway upregulated CD146 in human AF cells. Further investigation is needed to clarify the dual function of ERK in the regulation of CD146.

The limitations of the current study remain in the following aspects: This study investigated the effect of CD146 only on cell contractility and AF functional gene expression. Therefore, the roles of CD146 in other biological functions, such as cell migration, proliferation, differentiation, inflammation, and 3D ECM production warrant further investigation. The roles of SMADs and non-SMAD pathways in modulation of CD146 expression were only investigated by using shRNAs or inhibitors to eliminate the function of candidate pathways. It may be necessary to confirm our finding by over-expression of those key factors. So far, all studies of CD146+ cells for AF tissue engineering were performed in vitro, hence further in vivo studies are needed.

In conclusion, CD146 expression in AF cells was significantly upregulated by TGF-β1 in vitro, a growth factor known to support the reparative capacity of AF cells. CD146 is crucial to maintain the AF cell phenotype, by regulating several AF markers and cell
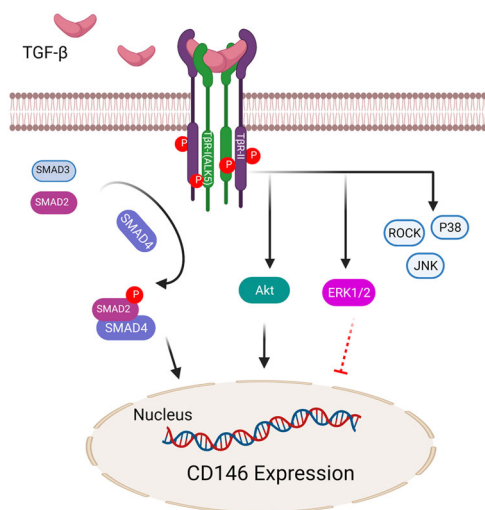
FIGURE 6 Conceptual model of signaling pathways of TGF-β-induced CD146 upregulation. TGF-β upregulate CD146 via TGF type I receptor, ALK5, and cascade canonical pathway SMAD2 and SMAD4, not SMAD3, and noncanonical pathway AKT, but not ROCK, JNK, and P38. ERK1/2 is a negative modulator of CD146 expression in protein level but not mRNA level. Created with BioRender. com. TGF-β, transforming growth factor-beta

contractility. Additionally, the present study demonstrated that the TGF-β induced CD146 expression in human AF cells, involves ALK5, SMAD2/4 and AKT signaling, and that ERK may be a negative modulator (Figure 6). Altogether, the findings from this study indicate that CD146 is a biomarker of functional AF cells and its regulation by TGF-β involves several pathways.

ACKNOWLEDGMENTS

AUTHOR CONTRIBUTIONS
Mauro Alini, Sibylle Grad, Laura B. Creemers, and Zhen Li contributed to the study design, Jie Du performed the experiments and wrote the manuscript, Wei Guo, Sonja Häckel, and Sven Hoppe helped with the experimental work. Marianna A. Tryfonidou, João P. Garcia, Laura B. Creemers, Sibylle Grad, Zhen Li, Wei Guo, and Sonja Häckel contributed to manuscript revision. All authors read and approved the final manuscript.

ORCID
Jie Du https://orcid.org/0000-0003-3400-9559
Mauro Alini https://orcid.org/0000-0002-0262-1412
Marianna A. Tryfonidou https://orcid.org/0000-0002-2333-7162
Sibylle Grad https://orcid.org/0000-0001-9552-3653
Zhen Li https://orcid.org/0000-0002-9754-6389

REFERENCES
1. Disease GBD, Injury I, Prevalence C. Global, regional, and national incidence, prevalence, and years lived with disability for 328 diseases and injuries for 195 countries, 1990-2016: a systematic analysis for the Global Burden of Disease Study 2016. *Lancet*. 2017; 390:1211-1259.
2. Iatridis JC, Michalek AJ, Purmessur D, Korecki CL. Localized intervertebral disc injury leads to organ level changes in structure, cellularity, and biosynthesis. *Cell Mol Bioeng*. 2009;2:437-447.
3. Alexeev D, Cui S, Grad S, Li Z, Ferguson SJ. Mechanical and biological characterization of a composite annulus fibrosus repair strategy in an endplate delamination model. *JOR Spine*. 2020;3(4): e1107.
4. Carragee EJ, Han MY, Suen PW, Kim D. Clinical outcomes after lumbar discectomy for sciatica: the effects of fragment type and anular competence. *J Bone Joint Surg Am*. 2003;85-A:102-108.
5. Ambrossi GL, McGirt MJ, Sciubba DM, et al. Recurrent lumbar disc herniation after single-level lumbar discectomy: incidence and health care cost analysis. *Neurosurgery*. 2009;65:574-578. discussion 578.
6. Smith JS, Ogden AT, Shafizadeh S, Fessler RG. Clinical outcomes after microendoscopic discectomy for recurrent lumbar disc herniation. *J Spinal Disord Tech*. 2010;23:30-34.
7. Guterl CC, See EY, Blanquer SB, et al. Challenges and strategies in the repair of ruptured annulus fibrosus. *Eur Cell Mater*. 2013;25: 1-21.
8. Nerurkar NL, Elliott DM, Mauck RL. Mechanics of oriented electrospun nanofibrous scaffolds for annulus fibrosus tissue engineering. *J Orthop Res*. 2007;25:1018-1028.
9. Christiani TR, Baroncini E, Stanzione J, Vernengo AJ. In vitro evaluation of 3D printed polycaprolactone scaffolds with angle-ply architecture for annulus fibrosus tissue engineering. *Regen Biomater*. 2019;6:175-184.
10. Nakai T, Sakai D, Nakamura Y, et al. CD146 defines commitment of cultured annulus fibrosus cells to express a contractile phenotype. *J Orthop Res*. 2016;34:1361-1372.
11. Takeoka Y, Yurube T, Morimoto K, et al. Reduced nucleotomy-induced intervertebral disc disruption through spontaneous spheroid formation by the Low Adhesive Scaffold Collagen (LASCol). *Biomaterials*. 2020;235:119781.
12. Schubert AK, Smink J, Arp M, Ringe J, Hegewald A, Sittinger M. Quality assessment of surgical disc samples discriminates human annulus fibrosus and nucleus pulposus on tissue and molecular level. *Int J Mol Sci*. 2018;19:19.
13. Lehmann JM, Holzmann B, Breitbart EW, Schmiegelow P, Riethmüller G, Johnson JP. Discrimination between benign and malignant cells of melanocytic lineage by two novel antigens, a glycoprotein with a molecular weight of 113,000 and a protein with a molecular weight of 76,000. *Cancer Res*. 1987;47:841-845.
14. Trzpis M, McLaughlin PM, de Leij LM, Harmsen MC. Epithelial cell adhesion molecule: more than a carcinoma marker and adhesion molecule. *Am J Pathol*. 2007;171:386-395.
15. Aplin AE, Howe AK, Juliano RL. Cell adhesion molecules, signal transduction and cell growth. *Curr Opin Cell Biol*. 1999;11:737-744.
16. Wang Z, Xu Q, Zhang N, Du X, Xu G, Yan X. CD146, from a melanoma cell adhesion molecule to a signaling receptor. *Signal Transduct Target Ther*. 2020;5:148.
17. Bardin N, George F, Mutin M, et al. S-Endo 1, a pan-endothelial monoclonal antibody recognizing a novel human endothelial antigen. *Tissue Antigens*. 1996;48:531-539.
18. Bardin N, Anfosso F, Massé JM, et al. Identification of CD146 as a component of the endothelial junction involved in the control of cell-cell cohesion. *Blood*. 2001;98:3677-3684.
19. Pickl WF, Majdic O, Fischer GF, et al. MUC18/MCAM (CD146), an activation antigen of human T lymphocytes. *J Immunol*. 1997;158: 2107-2115.

20. Espagnolle N, Guilloton F, Deschaseaux F, Gadelorge M, Sensébé L, Bourin P. CD146 expression on mesenchymal stem cells is associated with their vascular smooth muscle commitment. *J Cell Mol Med*. 2014;18:104-114.

21. Harkness L, Zaher W, Ditzel N, Isa A, Kassem M. CD146/MCAM defines functionality of human bone marrow stromal stem cell populations. *Stem Cell Res Ther*. 2016;7:4.

22. Leroyer AS, Blin MG, Bachelier R, Bardin N, Blot-Chabaud M, Dignat-George F. CD146 (Cluster of Differentiation 146). *Arterioscler Thromb Vasc Biol*. 2019;39:1026-1033.

23. Zabouo G, Imbert AM, Jacquemier J, et al. CD146 expression is associated with a poor prognosis in human breast tumors and with enhanced motility in breast cancer cell lines. *Breast Cancer Res*. 2009; 11:R1.

24. Zhang X, Wang Z, Kang Y, Li X, Ma X, Ma L. MCAM expression is associated with poor prognosis in non-small cell lung cancer. *Clin Transl Oncol*. 2014;16:178-183.

25. Onisim A, Vlad C, Simon I, Dina C, Achimas Cadariu P. The role of CD146 in serous ovarian carcinoma. *J BUON*. 2019;24: 1009-1019.

26. Du J, Long RG, Nakai T, et al. Functional cell phenotype induction with TGF-beta1 and collagen-polyurethane scaffold for annulus fibrosus rupture repair. *Eur Cell Mater*. 2020;39:1-17.

27. Yang H, Zhang L, Weakley SM, Lin PH, Yao Q, Chen C. Transforming growth factor-beta increases the expression of vascular smooth muscle cell markers in human multi-lineage progenitor cells. *Med Sci Monit*. 2011;17:BR55-BR61.

28. Ma Y, Zhang H, Xiong C, et al. CD146 mediates an E-cadherin-to-N-cadherin switch during TGF-beta signaling-induced epithelial-mesenchymal transition. *Cancer Lett*. 2018;430:201-214.

29. Williams B, Schneider RJ, Jamal S. Akt and PI3K-dependent but CREB-independent upregulation of MCAM by endothelin-3 in human melanocytes. *Melanoma Res*. 2014;24:404-407.

30. Tang X, Chen X, Xu Y, et al. CD166 positively regulates MCAM via inhibition to ubiquitin E3 ligases Smurf1 and betaTrCP through PI3K/AKT and c-Raf/MEK/ERK signaling in Bel-7402 hepatocellular carcinoma cells. *Cell Signal*. 2015;27:1694-1702.

31. Ercan D, Xu C, Yanagita M, et al. Reactivation of ERK signaling causes resistance to EGFR kinase inhibitors. *Cancer Discov*. 2012;2: 934-947.

32. Alzayadneh EM, Chappell MC. Angiotensin-(1-7) abolishes AGE-induced cellular hypertrophy and myofibroblast transformation via inhibition of ERK1/2. *Cell Signal*. 2014;26:3027-3035.

33. Kuma Y, Sabio G, Bain J, Shpiro N, Márquez R, Cuenda A. BIRB796 inhibits all p38 MAPK isoforms in vitro and in vivo. *J Biol Chem*. 2005;280:19472-19479.

34. Chen N, Fang W, Zhan J, et al. Upregulation of PD-L1 by EGFR activation mediates the immune escape in EGFR-driven NSCLC: implication for optional immune targeted therapy for NSCLC patients with EGFR mutation. *J Thorac Oncol*. 2015;10:910-923.

35. Balko JM, Schwarz LJ, Bhola NE, et al. Activation of MAPK pathways due to DUSP4 loss promotes cancer stem cell-like phenotypes in basal-like breast cancer. *Cancer Res*. 2013;73:6346-6358.

36. Jinnin M, Ihn H, Tamaki K. Characterization of SIS3, a novel specific inhibitor of Smad3, and its effect on transforming growth factor-beta1-induced extracellular matrix expression. *Mol Pharmacol*. 2006;69: 597-607.

37. Nakahara T, Moriuchi H, Yunoki M, Sakamato K, Ishii K. Y-27632 potentiates relaxant effects of beta 2-adrenoceptor agonists in bovine tracheal smooth muscle. *Eur J Pharmacol*. 2000;389:103-106.

38. Bowles RD, Williams RM, Zipfel WR, Bonassar LJ. Self-assembly of aligned tissue-engineered annulus fibrosus and intervertebral disc composite via collagen gel contraction. *Tissue Eng Part A*. 2010;16: 1339-1348.

39. Han M, Dong LH, Zheng B, Shi JH, Wen JK, Cheng Y. Smooth muscle 22 alpha maintains the differentiated phenotype of vascular smooth muscle cells by inducing filamentous actin bundling. *Life Sci*. 2009; 84:394-401.

40. Cs-Szabo G, Ragasa-San Juan D, Turumella V, Masuda K, Thonar EJ, An HS. Changes in mRNA and protein levels of proteoglycans of the anulus fibrosus and nucleus pulposus during intervertebral disc degeneration. *Spine*. 2002;27:2212-2219.

41. Schweitzer R, Chyung JH, Murtaugh LC, et al. Analysis of the tendon cell fate using Scleraxis, a specific marker for tendons and ligaments. *Development*. 2001;128:3855-3866.

42. Murchison ND, Price BA, Conner DA, et al. Regulation of tendon differentiation by scleraxis distinguishes force-transmitting tendons from muscle-anchoring tendons. *Development*. 2007;134:2697-2708.

43. Yoshimoto Y, Takimoto A, Watanabe H, Hiraki Y, Kondoh G, Shukunami C. Scleraxis is required for maturation of tissue domains for proper integration of the musculoskeletal system. *Sci Rep*. 2017;7:45010.

44. Hsieh CF, Yan Z, Schumann R, et al. In vitro comparison of 2D-cell culture and 3D-cell sheets of scleraxis-programmed bone marrow derived mesenchymal stem cells to primary tendon stem/progenitor cells for tendon repair. *Int J Mol Sci*. 2018;19:19.

45. Gumucio JP, Schonk MM, Kharaz YA, Comerford E, Mendias CL. Scleraxis is required for the growth of adult tendons in response to mechanical loading. *JCI Insight*. 2020;5:5.

46. Lee CH, Lee FY, Tarafder S, et al. Harnessing endogenous stem/progenitor cells for tendon regeneration. *J Clin Invest*. 2015;125:2690-2701.

47. Torre OM, Mroz V, Benitez ARM, Huang AH, Iatridis JC. Neonatal annulus fibrosus regeneration occurs via recruitment and proliferation of Scleraxis-lineage cells. *NPJ Regen Med*. 2019;4:23.

48. Belair DG, Whisler JA, Valdez J, et al. Human vascular tissue models formed from human induced pluripotent stem cell derived endothelial cells. *Stem Cell Rev Rep*. 2015;11:511-525.

49. Simon GC, Martin RJ, Smith S, et al. Up-regulation of MUC18 in airway epithelial cells by IL-13: implications in bacterial adherence. *Am J Respir Cell Mol Biol*. 2011;44:606-613.

50. Hill CS. Transcriptional control by the SMADs. *Cold Spring Harb Perspect Biol*. 2016;8:8.

51. Zhang YE. Non-Smad signaling pathways of the TGF-beta family. *Cold Spring Harb Perspect Biol*. 2017;9:9.

52. Lebrin F, Goumans MJ, Jonker L, et al. Endoglin promotes endothelial cell proliferation and TGF-beta/ALK1 signal transduction. *EMBO J*. 2004;23:4018-4028.

53. Feng XH, Derynck R. Specificity and versatility in tgf-beta signaling through Smads. *Annu Rev Cell Dev Biol*. 2005;21:659-693.

SUPPORTING INFORMATION

Additional supporting information may be found in the online version of the article at the publisher's website.